SEPTEMBER — OCTOBER 2021

OPTICAL EMISSION ANALYSIS OF ATMOSPHERIC PRESSURE METHANE PLASMA CHEMICAL VAPOR DEPOSITION

Y.-C. Chang, P.-Y. Wu, J.-C. Jhuang, C. Huang*

Department of Chemical Engineering & Materials Science, Yuan Ze University, Chung-Li, 32003, Taiwan; e-mail: chunhuang@saturn.yzu.edu.tw

The distinctive glow features of low-temperature RF CH₄/Ar plasma chemical vapor deposition and its correlation with plasma-deposited film characterizations were investigated. The optical emission spectroscopy diagnosis data and deposition results clearly indicated that, during CH₄/Ar glow discharge, the CH and C_2 species resulted from the low-energy electron-impact dissociation of CH₄ molecules that formed the deposition species, but the strong Ar emission lines were related to non-deposition species such as the argon atom. The results of the optical emission analysis indicated that the possible contribution of atmospheric pressure plasma-deposited film growth occurs primarily owing to a combination of electron-impact-dissociation and ionization.

Keywords: atmospheric pressure plasma, chemical vapor deposition, film growth, optical emission.

ОПТИКО-ЭМИССИОННЫЙ АНАЛИЗ ХИМИЧЕСКОГО ОСАЖДЕНИЯ ИЗ ПАРОВОЙ ФАЗЫ ПЛАЗМЫ МЕТАНА АТМОСФЕРНОГО ДАВЛЕНИЯ

Y.-C. Chang, P.-Y. Wu, J.-C. Jhuang, C. Huang*

УДК 543.423

Университет Юань Цзе, Чунг-Ли, 32003, Тайвань; e-mail: chunhuang@saturn.yzu.edu.tw

(Поступила 19 августа 2020)

Исследованы характерные особенности свечения при низкотемпературном высокочастотном плазмохимическом осаждении из газовой фазы в среде CH_4/Ar и его корреляция с характеристиками пленки, полученной плазменным напылением. Данные диагностики оптической эмиссионной спектроскопии и результаты осаждения показали, что во время тлеющего разряда CH_4/Ar частицы CH_4 и C_2 возникают в результате диссоциации молекул CH_4 под действием электронов низкой энергии, которые образуют частицы осаждения. Однако сильные линии излучения Ar связаны с неосажденными частицами, такими как атом аргона. Результаты оптико-эмиссионного анализа показали, что возможный вклад в рост пленки, осажденной плазмой атмосферного давления, происходит в первую очередь за счет комбинации диссоциации электронным ударом и ионизации.

Ключевые слова: плазма атмосферного давления, химическое осаждение из газовой фазы, рост пленки, оптическая эмиссия.

Introduction. Hydrocarbon films have attracted significant attention for various devices in industrial applications, including diffusion barriers, optical devices, anti-wetting surfaces, and biocompatible protective layers [1–4]. The low-temperature plasma chemical vapor deposition process is usually used in the fabrication of hydrocarbon thin films. Hydrocarbon film growth using low-temperature plasma chemical vapor deposition method, which uses partially ionized gases, is an alternative to conventional and/or traditional chemical vapor deposition methods. Low-temperature plasma, which can be easily created at low-pressure (e.g., <10 torr) by applying an electrical field, contains a large number of reactive species, including various

atoms, ions, energetic electrons, and UV irradiation. Despite their excellent deposition effectiveness, currently available plasma chemical vapor deposition processes have several restrictions, such as the limited volume of the plasma reactor and the additional vacuum and chemical cycles required. To address the limitations of low-pressure plasmas, various nonthermal atmospheric pressure plasma sources have been developed since the late 1980s [5]. Atmospheric pressure plasma, which is operated at a pressure of 1 atm, has many advantages for the development of manufacturing production processes, such as no need for vacuum equipment and its ease of operation. From this perspective, atmospheric plasmas possess some of the reactive characteristics of low-pressure plasmas. Therefore, atmospheric pressure plasmas can be used for deposition processes and are considered as a potential and promising alternative to conventional chemical vapor deposition techniques [6–10]. Different types of such plasmas can be created, including dielectric barrier discharge [11], corona discharge [12], resistive barrier discharge [13], and atmospheric pressure plasma jets sustained by radio frequency (RF) or microwave [14].

Although the optimization of the deposition process of hydrocarbon plasma chemical vapor deposition is usually achieved by practical methods, the influence of the luminous gas phase in the hydrocarbon plasma chemical vapor deposition system has not been precisely described. In a plasma glow discharge, the location of the luminous glow represents the electron energy level that is present [15–17]. Because of this aspect, the glow characteristics in plasma chemical vapor deposition have significant implications for understanding the creation mechanisms of chemically reactive species in plasma deposition. The hydrocarbon thin film deposition in plasma has been recognized as the atomic process to form the materials by breaking the bonding of organic monomers from the ion bombardment of the plasma state. This means that the monomer used in plasma chemical vapor deposition does not have to contain the functional groups. From this perspective, methane (CH₄), which contains only single bonds, was chosen as the monomer to study the atmospheric pressure (AP) plasma chemical vapor deposition process. Various low-pressure methane plasma deposition techniques that are employed to deposit hydrocarbon films, especially in diamond-like films, have been studied, such as direct current glow discharges, RF discharges, microwave glow discharges, and hollow cathode discharges [18]. However, there are only a few reports on atmospheric pressure methane plasma chemical vapor deposition [19]. Photo-emitting species are important in the luminous gas phase, and the location of the luminous gas phase indicates where the chemically reactive species reaction occurs with the inter-electrode space [20]. To distinguish the photo-emitting species, and thus indirectly determine the chemical composition of the glow in the atmospheric pressure methane plasma chemical vapor deposition system, an optical emission spectrometry (OES) was used as plasma diagnostic. The objective of this study is to characterize the glow formation, optical emission feature, and the film deposition in atmospheric pressure methane (CH₄) plasma chemical vapor deposition.

Experimental procedure. The plasma chemical vapor deposition was conducted using an atmospheric pressure plasma system that consists of a plasma jet and movable table, as shown in Fig. 1. The unfavorable plasma-deposited polymer coating is easily created inside of the gas channel of the atmospheric pressure plasma system. To address this disadvantage, a double-pipe-type quartz tube is used as the innovative gas channel of plasma jet, through which various gases flow at controllable flow rates [21]. For this design, monomer and carrier gas do not interfere with the plasma deposition because the quartz capillary acts as a barrier. The high-speed gas flow rate argon (4 slm/4000 sccm) is introduced from the upper side of the plasma system and passes through the quartz capillary as the ionization gas. The monomer is guided in the plasma system through the annular space between the quartz tube and the capillary. An electrical field is applied to the two electrodes located inside the quartz tube to ignite the plasma glow discharge using a 13.56-MHz RF power supply. Moreover, Fig. 1 also shows the luminous gas phase of this atmospheric pressure plasma jet. As the gas flow rate increases, the temperature of the atmospheric pressure plasma decreases further and approaches room temperature. The major plasma diagnostic apparatus of atmospheric pressure plasma jet is an optical emission spectroscopy. This equipment consists of both the instrumentation and spectrum analysis software, which was supplied by Hong-Ming Technology, Inc. The observable spectral range was 250-950 nm with a resolution of 2 nm. The grating is 600 lines/mm. A 1-m-long fiber optic cable was coupled to a fixed width (50 μm) slit. The chemical composition of atmospheric pressure plasma deposited hydrocarbon films was investigated using an X-ray photoelectron spectroscope (XPS) with the Mg K_{α} source (1253.6 eV).

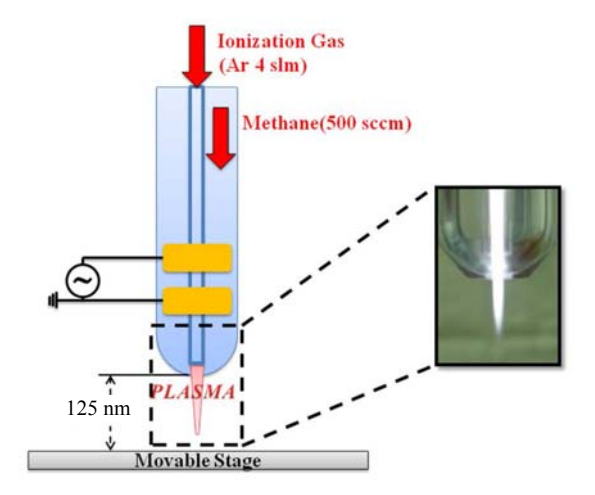


Fig. 1. Schematic diagram of the atmospheric-pressure plasma jet.

Results and discussion. Figure 2 shows the luminous gas phases in atmospheric pressure Ar plasma and atmospheric pressure Ar+CH₄ plasma in the same plasma system. It clearly shows the stable and characteristic plume-shaped glow discharge in dark space. In Fig. 2a, the luminous gas phase in atmospheric pressure plasma glow discharge of argon was surrounded by dark space and a well recognizable plume-shaped glow, which was present some distance from the nozzle. Therefore, in an atmospheric pressure plasma glow discharge of argon, the glow that appeared away from the nozzle can be attributed to the high-energy ionization of the argon species. In other words, a plume-shaped glow can be considered as a high-energy glow, which is caused by electrons having sufficiently high energy to ionize ground state Ar atoms. In contrast to the atmospheric pressure plasma glow discharge of argon, in the atmospheric pressure plasma glow discharge of hydrocarbon monomers such as methane, the dominant funnel-shaped glow forms at the center, and the plume-shaped glow as the secondary glow appears some distance away from the nozzle in Fig. 2b. The color change of the plume-shaped glow can be considered low-energy glow, whose energy is at the level of the dissociation energy of bonds involved in a hydrocarbon molecule and can be designated as a molecular dissociation glow. Because the low-energy electron in the cathode fall region can become energetic enough to dissociate an organic molecule long before it acquires enough energy to ionize the vapor, it is preferred that dissociation occur instead of ionization in plasma deposition [22]. The luminous gas phase in atmospheric pressure plasma is related to the nature of monomers and carrier gases. Inert gases such as Ar do not form molecular dissociate glow; the hydrocarbon monomer alters the basic glow characteristics in the atmospheric pressure plasma chemical vapor deposition system. It can be clearly observed that the effect of adding argon to the atmospheric pressure plasma glow discharge of a hydrocarbon monomer such as methane is to make the glow intensity and the glow volume different from that of a pure argon glow discharge. The glow intensity becomes much stronger, and the glow volume extends in the atmospheric pressure plasma glow discharge of argon because Ar only generates a high-energy glow. Moreover, both of the glow characteristics that appeared in the luminous phase of the atmospheric pressure plasma chemical vapor deposition system show that for the gaseous mixture, there was dissociation as well as ionization in the plasma state.

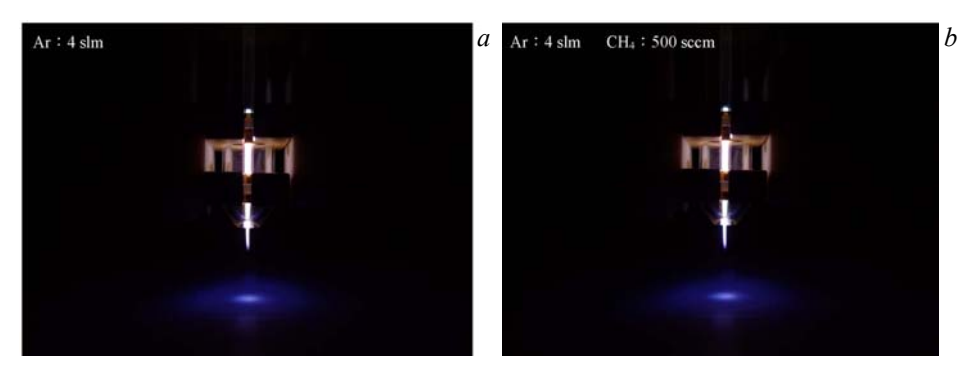


Fig. 2. Luminous gas phases of atmospheric pressure argon (a) and methane (b) plasma.

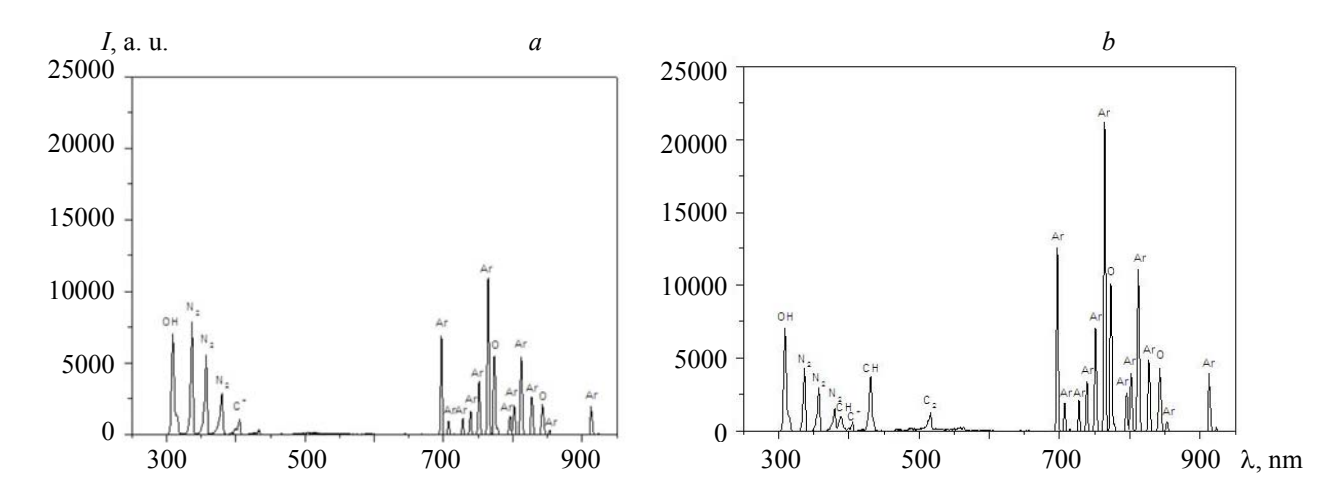


Fig. 3. Optical emission spectra obtained from atmospheric pressure argon (a) plasma and methane (b) plasma.

OES was used to monitor the excited plasma reactive species generated by the luminous gas phase of atmospheric pressure plasma. The photo-emitting species are significantly essential in the luminous gas phase, and the location of the luminous gas phase indicates where the chemically reactive species reaction occurs [23]. OES analysis is expected to explain the plasma reactive species that may contribute to atmospheric pressure plasma chemical vapor deposition. The typical emission spectra of atmospheric pressure Ar plasma and atmospheric pressure Ar+CH₄ plasma are shown in Fig. 3 from 300–900 nm, with no significant emissions outside of this region observed over the 200–1050-nm range of the instrument. The major intense emission lines that were observed in atmospheric pressure plasmas are list in Table 1. From Fig. 3, it can be noted that the feature of optical emission in atmospheric pressure Ar plasma is somewhat different from that in atmospheric pressure Ar+CH₄ plasma. From the OES spectra shown in Fig. 3a, the strong excited argon emission lines are observed at about 700-800 nm. The obvious emission line of the molecular nitrogen bands between 300-400 nm is also exhibited in optical emission spectra, as well as the emission line of the oxygen atom at 777 and 844 nm from the ambient air. Based on the optical spectra of atmospheric pressure Ar plasma, this corresponds to the possible reaction mechanism of Ar, N, and O plasma species. In addition, the primary photo-emission from atmospheric pressure Ar+CH₄ plasma in Fig. 3b represents Ar emission lines and are nondepositable. From the OES spectra shown in Fig. 3b, the photoemission of CH free radicals that can contribute to plasma deposition also appeared in atmospheric pressure Ar+CH₄ plasma. There were significant differences among these three types of low-temperature plasmas. The rotational band of 431.5 nm

TABLE 1. Most Intense Emission Lines Observed in Atmospheric Pressure Methane Plasma

Species	Transitions	Excitation energy, eV	Wavelength, nm
СН	$B^2\Sigma^-\leftarrow X^2\Pi$	_	388.9
	$A^2 \Delta, \nu = 0 \rightarrow X^2 \Pi, \nu = 0$	<11	431.4
C^+	$4f;^{2,4}F \to 3d;^4D^0$	_	407.7
CH^+	$A^1\Pi, \nu = 1 \rightarrow X^1\Sigma^+, \nu = 0$	_	417.2
C_2	$d^3\Pi_{ m g}$ – $a^3\Pi_{ m u}$	2.4	516.5
О	$3p^5P \rightarrow 3s^5S^0$	10.74	777.4
	$3p^3P \rightarrow 3s^3S$	10.99	844.6
ОН	$A^2\Sigma^+ \to X^2\Pi$	_	308.9
N_2	$C^3\Pi_u \to B^3\Pi_g$	11.1	315.9, 337.1, 357.7
	$C^3\Pi_u \to B^3\Pi_g$	11.2	380.5
Ar	$4p'[1/2] \rightarrow 4s[3/2]$	_	696.5
	$4p'[3/2] \rightarrow 4s'[1/2]^0$	13.48	750.4

due to an $A^2\Delta - X^2\Pi$ (0, 0) transition had a strong intensity in atmospheric pressure Ar+CH₄ plasma. The low intensity of the emission derived from CH emission bands located at 386 nm-390 nm ($X^2\Pi \leftarrow B^2\Sigma^-$), CH⁺ line at 417.9 nm, and C₂ swan band system at 516.5 nm ($d^3\Pi_g - a^3\Pi_u$) was also observed. This supports the assumption that the plasma deposited hydrocarbon film growth results from the electron-impact-dissociation of hydrocarbon molecules [23, 24]. The dissociation of molecules produces photo-emitting and chemically reactive species such as CH radicals in plasma chemical vapor deposition. This further implies that in hydrocarbon plasma deposited film growth, the chemically reactive species are not only created by electron-impact-dissociation, which occurred at atmospheric pressure Ar+CH₄ plasma, but also by the ionization of argon gas with high-energy electrons.

Figure 4 shows the emission spectra of atmospheric pressure Ar+CH₄ plasmas as a function of the CH₄ gas flow rate. Most of the emissions, including those with peaks at CH emission bands, originated from the increase in the excitation of methane molecules. In addition, the weak emissions at 516.5 nm (C₂ swan band system, $d^3\Pi_g - a^3\Pi_u$) also appeared in OES spectra with a high methane gas flow rate. Their relatively low intensities indicate a low electron temperature in the plasma [25]. Figure 4 also displays the normalized emission intensities of major emissions as a function of the CH₄ gas flow rate. The CH emission intensities increased with increasing gas flow rate. Figure 5 refers to the dependence of the CH₄ gas flow rate on the normalized emission intensities of nitrogen and oxygen emission lines from excited ambient air. The normalized emission intensities of nitrogen and oxygen emission lines decreased with increasing CH₄ gas flow rate, demonstrating a possible competition of plasma source gas and ambient air. In Fig. 5 the normalized emission intensities of argon emission lines is also shown. These stable normalized emission intensities can be considered to correspond to the ionization efficiency in the plasma, and it is stabilized with increasing CH₄ gas flow rate as well. Figure 6 shows the emission spectra in the atmospheric pressure Ar+CH₄ mixture gas plasma as a function of the RF plasma power. As shown in Fig. 6, an increasing RF plasma power was applied to the Ar+CH₄ mixture discharge plasma system, whereas it increased the CH₄ gas flow rate of that to the same in Fig. 4. The emission intensities are seen to increase with increasing RF plasma power. The emission intensities increase with rising RF plasma power level, demonstrating an increase in the density of highly energized electrons. Ion bombardments were more reactive in atmospheric pressure Ar+CH₄ mixture gas plasma system with increasing RF plasma power because of the higher energy input of the electric field. The normalized emission intensities of the major emission lines in Fig. 7 were markedly weaker than that in Fig. 6, which indicates that Ar emission lines decreased with increase in RF plasma power. This may be due to the rapid consumption in the Ar+CH₄ mixture at excessive energy in gas channels. CH emission lines as well as the C₂ Swan band should also occur in the peak more weakly as the RF plasma power increase; on the contrary, experiment results showed that the C₂ Swan band of atmospheric pressure Ar+CH₄ mixture gas plasma occurred more strongly as the RF plasma power increased, as shown in Fig. 7.

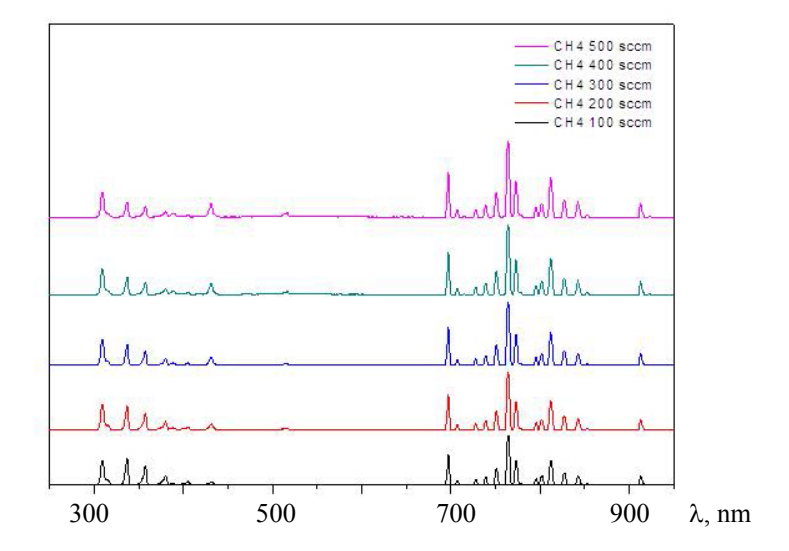


Fig. 4. Optical emission spectra of atmospheric pressure methane plasma with monomer gas flow rate inputs.

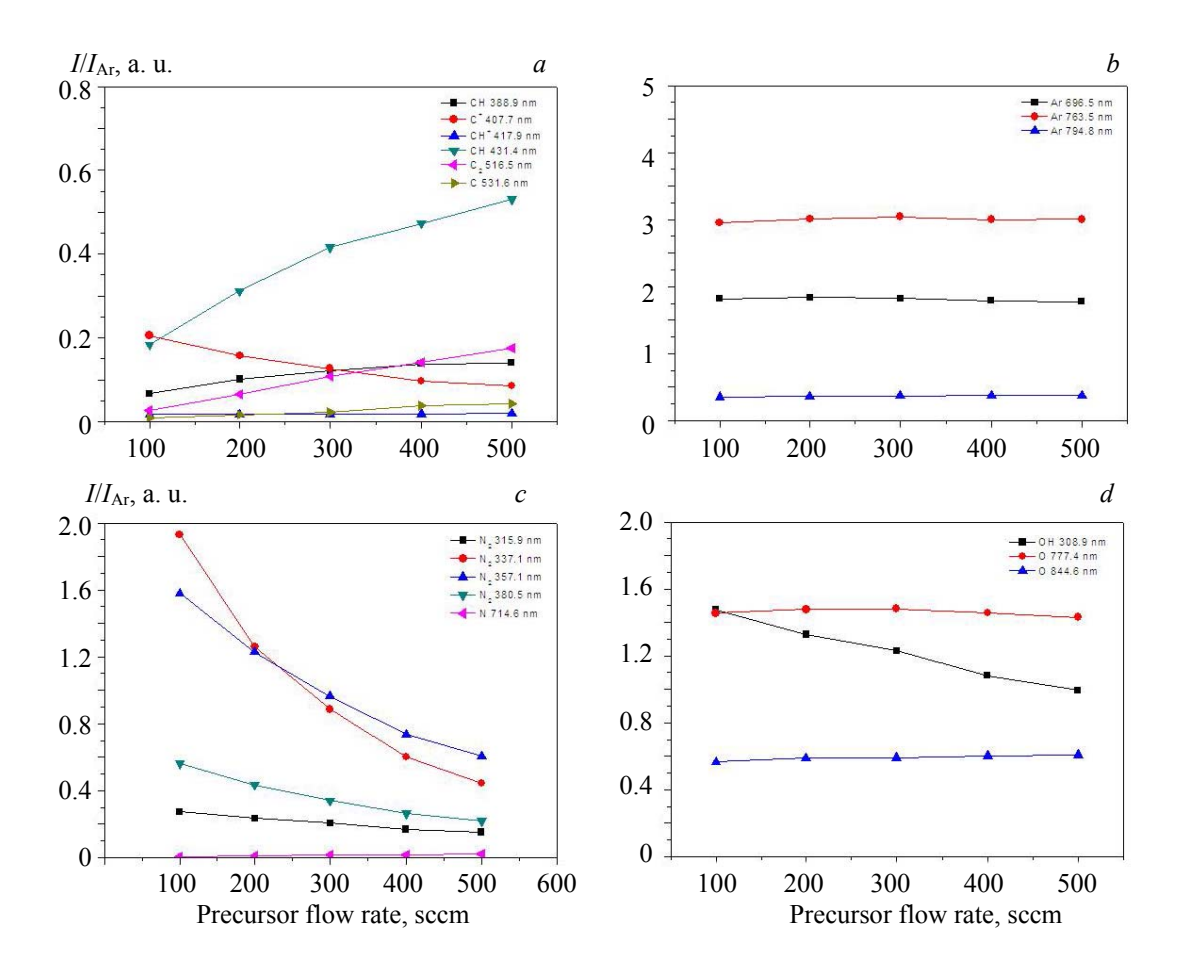


Fig. 5. Optical emission intensity dependence of (a) CH lines, (b) argon, (c) nitrogen, and (d) oxygen lines with monomer gas flow rate inputs.

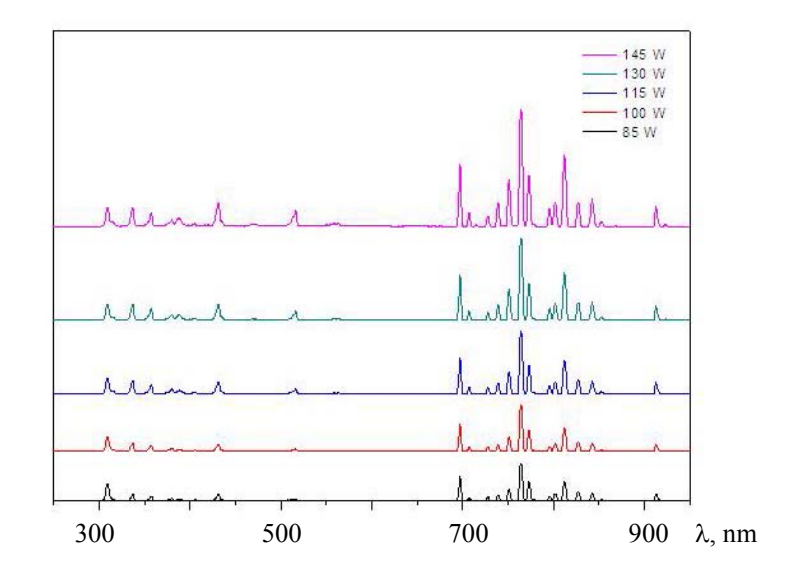


Fig. 6. Optical emission spectra of atmospheric pressure methane plasma with RF plasma power level inputs.

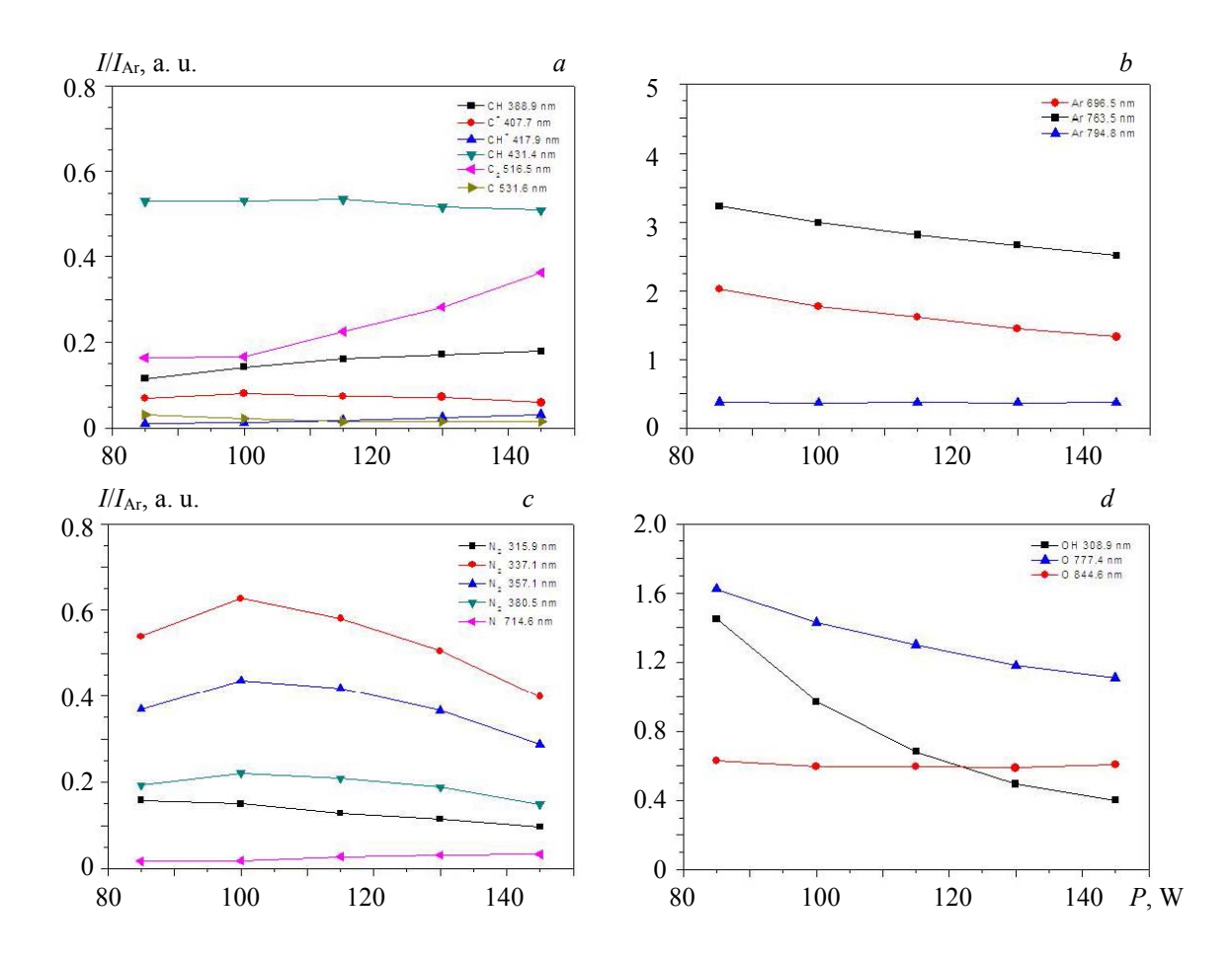


Fig. 7. Optical emission intensity dependence of (a) CH lines, (b) argon, (c) nitrogen, and (d) oxygen lines with RF plasma power level inputs.

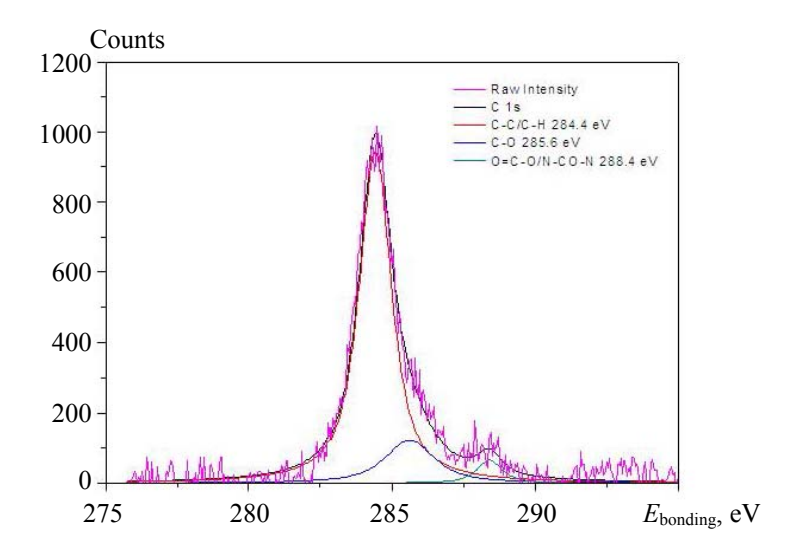


Fig. 8. XPS C1s spectra from atmospheric pressure methane plasma-deposited hydrocarbon film.

In atmospheric pressure $Ar+CH_4$ plasma chemical vapor deposition, CH radicals are formed directly from the methane monomer decomposition of the CH_x fragments by electron impact dissociation. As a re-

sult, it is assumed that CH_x radicals play a leading position in atmospheric pressure plasma deposited hydrocarbon film growth. This contribution is based on the fact that CH_x radicals have relatively long lifetimes (of the order of several milliseconds) in plasma [26, 27]. The atomic percentages of the carbon, oxygen, and nitrogen present in the atmospheric pressure plasma-deposited hydrocarbon films by XPS detection are follows: C – 66.9 at.%, O – 28.5 at.%, N – 4.7 at.%, O/C – 0.43 at.%. The atmospheric pressure plasma deposited hydrocarbon films comprised 66.9 at.% carbon, 28.5 at.% oxygen, and 4.6 at.% nitrogen. The presence of carbon in the film is believed to be due to the decomposition of the methane monomer. In order to evaluate the chemical compositions of atmospheric pressure plasma-deposited hydrocarbon films, XPS deconvolution analysis of C1s peaks was performed. As shown in Fig. 8, the C1s spectrum of atmospheric pressure plasma-deposited hydrocarbon film contained two distinct peaks at 284.4 and 285.6 eV, corresponding to C–C/C–H groups and C–O group. At the same time, additional peaks at 288.4 eV also appear, which could be attributable to –C–O/O — C — O groups [28–33]. XPS analysis results confirm that the possible contribution of plasma-deposited film growth occurred mainly with the combination of electron-impact-dissociation and ionization in atmospheric pressure Ar+CH₄ plasma by OES.

Conclusions. The influence of the luminous gas phase of glow discharge on the atmospheric pressure methane plasma chemical vapor deposition process was examined using the glow feature, optical emission spectra, and the film deposition. OES was used to detect the transition of luminous gas phases of Ar and Ar+CH₄ plasmas generated in a 1 atm air environment using a double-pipe-type plasma jet. From OES analysis, it is proved that the CH_x radicals are present during atmospheric pressure plasma chemical vapor deposition. The photoemission of CH_x radicals, which can contribute to deposition, appeared primarily in atmospheric pressure methane plasma chemical vapor deposition. This supports the assumption that methane plasma deposited a film growth on account of the electron-impact-dissociation of methane molecules. The low-energy electron in the process of gaining energy can become sufficiently energetic to dissociate an organic molecule (slow electron-impact dissociation). The increases in the CH emission intensities and intensity ratios with increasing CH₄ gas flow rate reveal the correlation of the amount of monomer input on the plasma deposition. However, the decrease in the nitrogen and oxygen emission intensity ratios should be considered when explaining the competition plasma source gas and ambient air. These results demonstrate that OES provides a useful approach to study the operational conditions and plasma chemistry. Our investigation clearly shows the dominant effects of luminous gas phases on the film-forming tendency in atmospheric pressure methane plasma chemical vapor deposition.

REFERENCES

- 1. Y. Kimura, D. Ishikawa, A. Nakano, A. Kobayashi, K. Matsushita, D. de Roest, N. Kobayashi, *Jpn. J. Appl. Phys.*, **51**, 05EC04 (2012).
- 2. M. Cappelli, T. Owano, C. Kruger, J. Mater. Res., 5, 2326 (1990).
- 3. S. Bugaev, A. Korotaev, K. Oskomov, N. Sochugov, Surf. Coatings Technol., 96, 123 (1997).
- 4. J. Kim, G. Liu, S. Kim, J. Mater. Chem., 16, 977 (2006).
- 5. S. Kumagai, H. Matsuyama, Y. Yokoyama, M. Hori, M. Sasaki, Jpn. J. Appl. Phys., 50, 08JA02 (2011).
- 6. H. Kakiuchi, H. Ohmi, Y. Kuwahara, M. Matsumoto, Y. Ebata, K. Yasutake, K. Yoshii, Y. Mori, *Jpn. J. Appl. Phys.*, **45**, 3587 (2006)
- 7. J. Albaugh, C. O'Sullivan, L. O'Neill, Surf. Coatings Technol., 203, 844 (2008).
- 8. H. Ohmi, H. Kakiuchi, N. Tawara, T. Wakamiya, T. Shimura, H. Watanabe, K. Yasutake, *Jpn. J. Appl. Phys.*, 45, 8424 (2006).
- 9. Y. J. Chang, C. H. Lin, C. Huang, Jpn. J. Appl. Phys., 55, 01AB05 (2016).
- 10. W. C. Ma, C. H. Lin, C. Huang, *Plasma Proc. Polym.*, **12**, 362 (2015).
- 11. M. Nishida, K. Yukimura, S. Kambara, T. Maruyama, Jpn. J. Appl. Phys., 40, 1114 (2001).
- 12. F. Tochikubo, H. Arai, Jpn. J. Appl. Phys., 41, 844 (2002).
- 13. M. Laroussi, *IEEE Trans. Plasma Sci.*, **30**, 1409 (2003)
- 14. H. Yoshiki, K. Ikeda, A. Wakaki, S. Togashi, K. Taniguchi, Y. Horiike, *Jpn. J. Appl. Phys.*, **42**, 4000 (2003)
- 15. M. H. Brodsky, M Cardona, J. J. Cuomo, *Phys. Rev. B*, **16**, 3556 (1977).
- 16. C. Huang, C. H. Liu, W. T. Hsu, T. H. Chou, J. Non-Cryst. Solids, 356, 1791 (2010).
- 17. W. C. Ma, C. Y. Tsai, C. Huang, Surf. Coatings Technol., 259, 290 (2014).

- 18. D. S. Bethune, C. H. Kiang, M. S. De Vries, G. Gorman, R. Savoy, J. Vazquez, R. Beyers, *Nature*, 363, 605 (1993).
- 19. S. L. Girshick, C. Li, B. W. Yu, H. Han, Plasma Chem. Plasma Proc., 13, 169 (1993).
- 20. L. Calin, A. Mihalcioiu, S. Das, V. Neamtu, C. Dragan, L. Dascalescu, A. Iuga, *IEEE Trans. Ind. Appl.*, 44, 1038 (2008).
- 21. D. W. Hutmacher, *Biomaterials*, **21**, 2529 (2000).
- 22. S. PalDey, S. C. Deevi, Mater. Sci. Eng. A, 342, 58 (2003).
- 23. I. Hamberg, C. G. Granqvist, J. Appl. Phys., 60, R123 (1986).
- 24. M. Hegelich, S. Karsch, G. Pretzler, D. Habs, K. Witte, W. Guenther, M. Allen, M. Roth, *Phys. Rev. Lett.*, **89**, 085002/1 (2002).
- 25. P. G. De Gennes, Phys. Rev., 118, 141 (1960).
- 26. L. J. Stern, J. H. Brown, T. S. Jardetzky, J. C. Gorga, R. G. Urban, J. L. Strominger, D. C. Wiley, *Nature*, **368**, 215 (1994).
- 27. R. Ahmed, D. Gray, Science, 272, 54 (1996).
- 28. I. B. Denysenko, S. Xu, J. D. Long, P. P. Rutkevych, N. A. Azarenkov, K. Ostrikov, *J. Appl. Phys.*, **95**, 2713 (2004).
- 29. N. Inagaki, S. Tasaka, K. Hibi, J. Polym. Sci. Polym. Chem., 30, 1425 (1992).
- 30. J. S. Kim, M. Granström, R. H. Friend, N. Johansson, W. R. Salaneck, R. Daik, W. J. Feast, F. Cacialli, *J. Appl. Phys.*, **84**, 6859 (1998).
- 31. C. Y. Tsai, R. S. Juang, C. Huang, Jpn. J. Appl. Phys., 50, 08KA02 (2011).
- 32. K. Takenaka, Y. Setsuhara, Jpn. J. Appl. Phys., 52, 11NE04 (2013).
- 33. F. Hempel, P. B. Davies, D. Loffhagen, L. Mechold, J. Röpcke, *Plasma Sour. Sci. Technol.*, **12**, S98 (2003).